LARGE-SCALE PV POWER PLANTS FOR MITIGATION CONTROL AGAINST PARTIAL SHADING EFFECTS

#1SHRIRAJ, PG STUDENT
#2RAMAKRISHNA P – ASSISTANT PROFESSOR
DEPT OF EEE
KITS COLLEGE - RAMACHANDRA PURAM

ABSTRACT—This study proposes a novel control strategy to allow partially shaded photovoltaic power plants (PV-PPs) to mitigate the detrimental effects on the frequency of power systems without the need for energy storage. The strategy divides the PV-PP into*N* sections operating in a deloaded mode with a specific reserve level. A central controller continually monitors each of these PV sections. When one or more sections are under shaded conditions, the control orders the unshaded sections to deploy their active power reserves to smooth the power output at the interconnection point of the PV-PP. The proposed control was tested in the isolated power system of northern Chile considering different PV scenarios and levels of deload. Results show that the control is effective in assisting frequency regulation, especially under large PV penetration scenarios. For these cases, and only on days with high irradiance variability, the benefits gained from the control strategy could be more valuable for the system than the forgone revenues due to the deloaded operation.

Index Terms—Control strategy, frequency control, partial shading, photovoltaic (PV) generation.

I. INTRODUCTION

T HE increasing construction of large-scale photovoltaic power plants (PV-PPs) over the past few years has led to considerable concern among transmission system operators (TSOs) largely due to frequency-related operational issues. The inherent variability and uncertainty of solar irradiation, as well as conventional operation at the maximum power point (MPP) of PV-PPs, necessarily lead to a reduction of the system's capability to deal with frequency deviations.

The output power of PV-PPs is variable in nature because of changes in the sun's position throughout the day and the seasons, as well as variable weather conditions. At sunset and sunrise, PV output power usually varies between 10% and 13% over a period of 15 min for single-axis tracking PV-PPs [1]. Considering the day-ahead power system operation planning, the solar geometry can be well forecasted and thus managed by TSOs. However, rapid changes in the output power of PV-PPs. due to moving clouds are driven by complex stochastic processes. Operating experience with large-scale PV-PPs shows that large and rapid fluctuations in solar irradiance, and thus in the output power of the PV-PPs, are possible in partly cloudy conditions [2]. The time it takes for a passing cloud to shade an entire PV-PP depends on the plant size, cloud speed, cloud height, and other factors [1]. For PV-PPs with rated capacities around 100 MW, this shading time is of the order of a few minutes. This is the case, for instance, in some PV-PPs in the Southwest U.S., where output power can change by more than 70% in 5–10 min on partly cloudy days [2], [3]. Depending on system operating conditions and PV penetration, such large and sudden changes in the output power of PV-PPs could exhaust the ramping reserves available in conventional generation units, and thus threaten the power balance in the system.

Moreover, under such circumstances, attempts of conventional power plants to follow the changes in the net load can lead to an increase in the cycling of synchronous generators, which could cause extra wear and tear on the generating equipment. This produces additional costs and reduced profit from the generator [4]. Several studies have reported that these frequency issues could constrain the integration of large-scale PV-PPs in power systems, especially in systems with slow secondary frequency response [5], or in isolated power systems due to the inherent low inertia and reduced capabilities for frequency regulation. The effects of partial shading in PV-PPs are well known and have been extensively studied over the past few years. The proposed solutions to extract maximum power from partially shaded PV arrays cover a wide range of possibilities, starting from modified MPP tracking techniques for detecting the global MPP to different array configurations for interconnecting PV modules [6]. Other alternatives include different PV system architectures and converter topologies. These investigations have focused on optimizing the operation of the PV-PP itself. Nevertheless, methods for mitigating the effects of partially shaded PV-PPs from a power system perspective have not been widely researched until now.

One main contribution of this study is to propose a novel control strategy to allow partially shaded PV-PPs to mitigate their negative effects on the system frequency without the need for an energy storage system. This control, denoted as "mitigation control against partial shading effects" (MICAPAS), was tested in the isolated power system of northern Chile considering different PV penetration levels. This paper is organized as follows. Section II summarizes the effects of partial shading conditions in PV-PPs. Section III describes existing solutions to maximize the power output of partial shaded PV arrays. Section IV presents the proposed

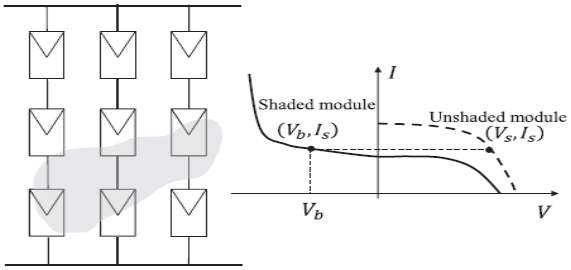

Fig. 1. Operation of a shaded PV-PP.

novel control strategy that allows partially shaded PV-PPs to mitigate the detrimental effects on the frequency of power systems. The case study is presented in Section V. Section VI shows the results obtained and Section VII draws the main conclusion of this research.

II. PARTIAL SHADING EFFECTS IN PV-PPS

Partial shading in large-scale PV-PPs, particularly in those occupying a wide area, is a common phenomenon that occurs when some panels within the PV-PP are completely or partially shaded by moving clouds. Partial shading has undesirable effects, such as reduction in the generated power from the PV-PP [7], [8] and hot spots inside the structure [6], [7], [9]–[12].

The shading condition leads to varying irradiation on different portions of the PV-PP. Since the short circuit current of a PV module is proportional to the solar insolation level, this leads to a reduction of the photocurrent for the shaded panel, while the unshaded modules continue their operation at a higher photocurrent [6]. As the current through all series-connected panels must be equal, the shaded modules must then operate in the reverse bias region, in order to be able to conduct the larger current of the unshaded panels (see Fig. 1) [6]. The shaded modules dissipate a part of the electric power generated by the unshaded modules in the form of heat (phenomenon known as hot spot) [9], [10], [13]. The presence of hot spots can irreversibly damage the PV modules [9]–[11], [14], especially when extreme shading situations lead to a reverse bias that exceeds the solar cell breakdown voltage [15].

Hot spot effects can be avoided using bypass diodes [6], [7], [10], [11], [13]–[17], which protect the modules from local heating. Indeed, in commercial PV modules a number of bypass diodes are connected across groups of PV cells to prevent the hot-spot phenomena [18]. Nevertheless, bypass diodes do not solve the problem of the reduction in the generated power of the PV-PP under partial shading conditions [7]. Moreover, these diodes create multiple power peaks, which increase the complexity of themaximum power point tracking (MPPT) technique [6], [7], [16]. The occurrence of multiple peaks can mislead the MPPT algorithms, trapping them at local peaks [8] due to their inability to discriminate between local and global power maximums [11], [17], [19]. Consequently, conventional tracking techniques, such as perturb and observe [20], hill climbing [21], ripple correlation [22], or power feedback control [23], are not suitable in these cases.

III. SOLUTIONS AGAINST PARTIALLY SHADED PV ARRAYS

In response to the aforementioned challenge of finding the global MPPT in partially shaded PV arrays, many techniques have been developed. References [6] and [24] provide a comprehensive summary of the available solutions, which can be organized into firmware and hardware approaches.

A. Global MPPT Based on Firmware

Firmware approaches consist of software controls with modified MPPT techniques including *two-step methods*, such as the system characteristic curve [25]–[27], power curve slope [28], and power increment method [29]. These approaches try to localize the approximate location of the global optimum in the first step and then use traditional MPPT methods to refine its exact location.

Segmental search methods split the operating range of the characteristic curve into smaller portions and gradually reduce the searching range by diverse methods, including the dividing rectangles [30] and Fibonacci methods [31], [32]. *Soft computing methods* are heuristics for computational intensive tasks. Finding the global MPPT can be understood as an optimization problem, accordingly such methods have been proposed to find

the optimal operation point, including artificial neural networks [33], particle swarm optimization [12], [34]– [36], fuzzy logic controls [37], chaos search [38], tabu search [39], cuckoo search [40], bee and ant colony [41], [42], modified differential evolution [43], and genetic algorithms [44].

Finally, there are *other methods* that do not fit into the previous categories; for example, the extreme seeking control [45] an adaptive closed-loop control, and the predictive control method [46] that uses weather forecasts to set the operation point. A critical review of firmware-based MPPT methods during partial shading is provided in [47].

B. Global MPPT Based on Hardware

These methods rely on different hardware configurations. It includes examining how alternative array connections, such as total-cross-ties or bridge links, help to cope with shading in contrast to the traditional series–parallel layout [48], [49].

Several studies analyze how different kinds of *systemarchitecture*, such as series-connected and parallel-connected microconverters and microinverters (distributed architecture) achieve higher power yield under shading than the standard centralized architectures [50], [51].

Further changes to the *circuit topology* of power electronics can be done to extract more power. Examples are using multilevel diode-clamped converters [52], modifying the operating voltage of PV modules via a generation control circuit [53], injecting a bias voltage into the shaded regions [54], additional circuitry to separate the current between the shaded

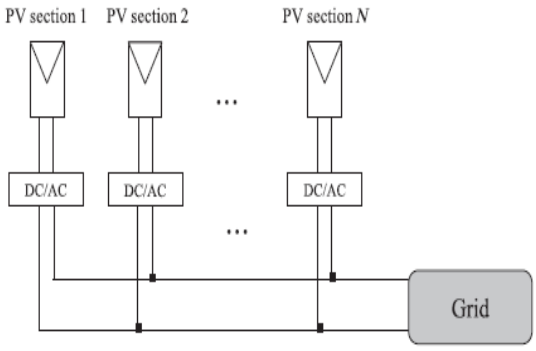

Fig. 2. Microinverter architecture

and unshaded modules [55], or employing module-integrated converters (dc/dc converter attached to each module) [56] or multiple input converters [57]. The goal of all the aforementioned methods is to maximize the output power of PV-PPs either by reducing the power losses or by improving the MPPT technique. Although this is important for power plant revenue, from a power system perspective, however, the output power of the PV-PP will still follow the irradiation's variability with the subsequent consequences on the frequency regulation. Thus, mitigation solutions from the power system perspective are essential for allowing massive levels of PV penetration.

IV. MITIGATION CONTROL AGAINST PARTIAL SHADING EFFECTS

The control strategy to allow partially shaded PV-PPs to mitigate the detrimental effects on system frequency is based on PV arrays operating below their optimal operation point (deloaded operation). The strategy divides the PV-PP into N sections, each section with a specific reserve level. This study considers that the reserve level in the PV-PPs is defined *a priori* by TSOs in order to ensure good performance of the frequency regulation of the system.

However, the allocation and quantification of the operating reserves by the TSO are not addressed in this paper. The control strategy (MICAPAS) requires a PV-PP architecture, in which the global MPP of individual PV sections can be tracked under partial shading conditions. Thus, a parallelconnected microconverter, series-connected microconverter, or a microinverter architecture are possible choices [6]. In this study, a microinverter architecture is employed; where each PV section can be composed of several panels (see Fig. 2).

A central controller is continually monitoring each PV section of the PV-PP. When one or more sections are under shaded conditions, the controller orders the unshaded sections to deploy their active power reserves, in order to smooth the power output at the point of interconnection of the power plant. A general block diagram of the control strategy is shown in Fig. 3. The block "reserve level calculation" in Fig. 3 estimates the total amount of operating reserves available in the PV-PP according to

$$R_t(\chi) = \sum_{i=1}^{N} P_i^{mpp}(E,T) \cdot \chi \qquad (1)$$

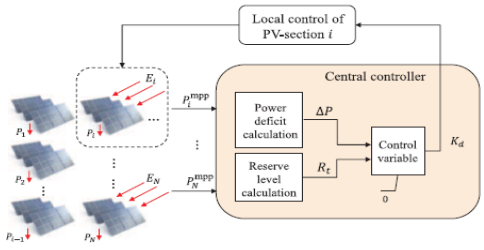

Fig. 3. General diagram of MICAPAS.

where *P*mpp *i* is the power of the PV section *i* at the MPP (for a determined temperature *T* and insolation *E*), and χ is the deload level defined *a priori* by the operator (with values between 0 and 1). The block "power deficit calculation" computes the total power shortage due to a shading situation based on

$$\Delta P = \left\{ \sum_{i=1}^{N} \max\left\{P_i^{mpp}\right\}_{i=1,\ldots,N} - P_i^{mpp} \right\} \cdot (1-\chi). \quad (2)$$

From (2), it can be seen that Δ*P* is different from zero only when at least one PV section is not under shading conditions, i.e., when at least one section is operating with a solar insolation level different from the rest of the power plant. If the PV-PP is totally shaded, Δ*P* will be zero and no control action will be undertaken.

Based on the power deficit and total reserves, the central controller defines a control signal (*Kd*) to command the deployment of the power reserves in case of a shading condition. This control signal is defined according to

$$K_d = \left(1 - \frac{\Delta P}{R_t(\chi)}\right). \qquad (3)$$

The signal *Kd* takes values between 0 (when the power deficit is equal to the total reserves) and 1 (when Δ*P* is zero).

If Δ*P* >*R*(χ), the value of *Kd* is limited to its lower value, 0. From a control viewpoint, two situations can occur

1) *Kd* = 1: No control action will be carried out and the deloaded operation of each PV section is sustained.

2) *Kd* < 1: The control signal will deploy the active power reserves of the PV-PP.

In this study, the deloaded operation of the PV section is accomplished by operating the array with a dc voltage lowerthan the optimal dc operation voltage, *V i*,mpp dc corresponding to the MPP. Although an increased dc voltage would also result in an output power reduction of the PV-PP, a reduced dc voltage is selected due to the higher efficiency of the converter [58].

The local control scheme of each PV section is implemented according to Fig. 4. In the figure, the *q*-axis has been omitted for simplicity. The deloaded operation is implemented by generating a supplementary control signal (Δ*V i*
dc). The difference between the actual value of the dc voltage (*V i* dc) and its optimal value (*V i*,mpp dc) is compared with this additional signal, and the

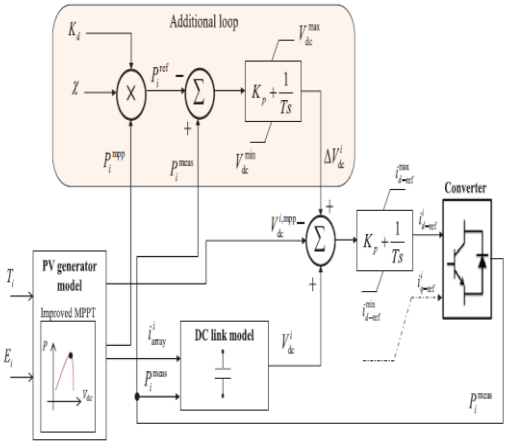

Fig. 4. Local control scheme for section *i* of the PV-PP.

error is sent to a PI controller thereafter. This PI control generates the reference value for the *d*-axis component of the current $(i_{d-\mathrm{ref}}^{i})$ that regulates the active power of the converter. The PI controller is limited by two parameters $i_{d-\mathrm{ref}}^{\min}$ and $i_{d-\mathrm{ref}}^{\max}$.

V. CASE STUDY

A. Power System Under Study: Northern Interconnected System (NIS) of Chile

To measure the performance of the proposed control strategy,the 50-Hz-isolated electricity system of northern Chile (NIS) was considered. The system is characterized by a thermal generation mix based on coal, oil, and natural gas with a projected installed capacity of 5800MWfor the year 2020. The projected peak load is 3300 MW. The system load is characterized by 90% of industrial load (mining industry), while the remaining 10% corresponds to residential customers.

The NIS is located in the middle of the Atacama Desert and, therefore, is a good example of a power system exhibiting an outstanding solar potential for PV projects. Nevertheless, some technical constraints related to its conventional generation units such as low inertia levels, limited ramp rates, and slow reaction times could hamper the network integration of PV-PPs due to frequency issues.

B. Considered PV Scenarios:

The study was conducted under two PV scenarios, namely:
1) S15 and 2) S25, with the total PV capacity for each scenario being 15% (890 MW) and 25% (1500 MW), respectively, of the total installed capacity of the system for the year 2020. The scenarios were constructed using available information of future PV projects corresponding to current private initiatives in Chile [59], [60].

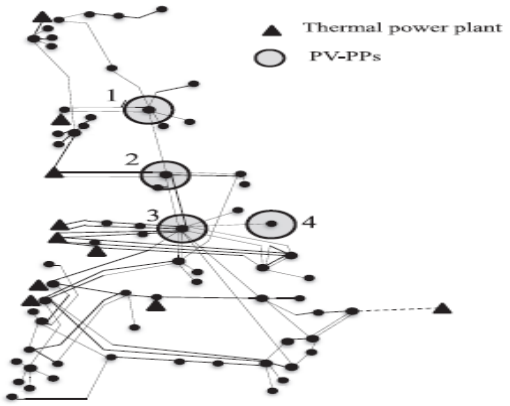

Fig. 5. Simplified diagram of the NIS of Chile.

The PV-PPs are distributed at four locations throughout the Atacama Desert. The network structure and the location of the PV power plants are shown in the simplified diagram of Fig. 5.

C. Modified Clear Sky Index

In order to test the performance of the MICAPAS, a critical day in terms of high solar variability was selected. To do this, a modified version of the clear sky index [2], [61], [62] was proposed. Considering an irradiation series with a time resolution of T = 10 min, the modified clear sky index (MCSI) for day $d*$ at location k is defined as

$$\mathrm{MCSI}_{d*}^{k} = \sum_{i=1}^{144} \frac{\left|\Delta \mathrm{SI}_{d*}^{k}(i) - \Delta \mathrm{SI}_{d*}^{k}(i-1)\right|}{T} \qquad (4)$$

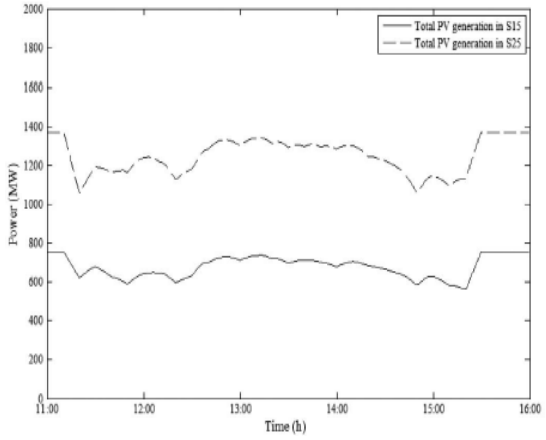

Fig. 6. Aggregated PV injections at February 5 for both scenarios.

$$\Delta \mathrm{SI}_{d*}^{k}(i) = \mathrm{SI}_{d*}^{k,\mathrm{ref}}(i) - SI_{d*}^{k,\mathrm{forec}}(i) \qquad (5)$$

where SIk,forec $d*$ (i) represents the ith sample of the forecasted solar radiation series at location k during the day $d*$ and SIk,forec $d*$ (i) is the ith sample of the irradiation at location k if the sky were clear. The MSCI is normalized by dividing by its maximum value during the day. The MCSI is an indicator of the variability of the irradiation during the day $d*$. The closer the value of the MCSI is to one, the more variable the irradiation during the day in question.

D. Simulated Day

The performance of the MICAPAS was tested for a critical day in terms of high solar variability. The critical day was identified based on available solar irradiation measurements for the year 2013. This day occurred on February 5, which is part of the *Bolivian Winter* phenomenon of the Atacama Desert. Fig. 6 shows the aggregated PV power injections for both scenarios between 11:00 A.M. and 16:00 P.M. on February 5.

The system demand is assumed constant in the study and equal to its average value for that day (2832 MW). This is justified due to the strong industrial load characteristics of the NIS demand (load factor close to one), which leads to a quite flat load profile during the year.

VI. OBTAINED RESULTS

A simplified model of the NIS with 120-buses for the year 2020 was implemented in the power system simulation tool DIgSILENT Power Factory [63]. The proposed control was simulated for the critical day considering three deload levels for PV-PPs: 5%, 10%, and 15%. For comparison purposes, a baseline with the MICAPAS inactive (deload level of 0%) was also simulated.

Figs. 7 and 8 present the system frequency for different deload levels in the PV-PPs for the scenarios S15 and S25, respectively. The straight line at 49.8 Hz indicates the lowest allowable level for the system frequency according to the Chilean grid code during normal operation. Table I shows the percentage of the time that the system frequency is below 49.8 Hz in each case.

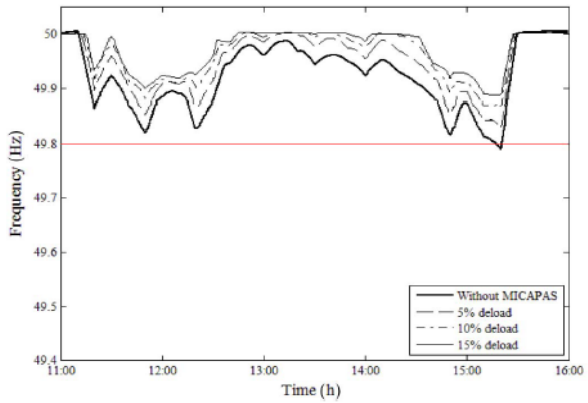

Fig. 7. System frequency in scenario S15.

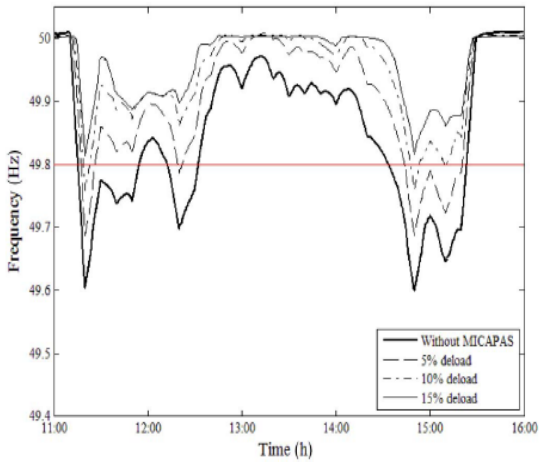

Fig. 8. System frequency in scenario S25.

TABLE I

AMOUNT OF TIME (%) THAT SYSTEM FREQUENCY IS BELOW 49.8 HZ FOR SCENARIO S15 AND S25

SCENARIO	WITHOUT MICAPAS	5% DELOAD	10% DELOAD	15% DELOAD
S15	1.0	0.0	0.0	0.0
S25	36.3	16.1	3.5	0.0

From Figs. 7 and 8, it can be concluded that the system frequency performance during normal operation degrades as the PV penetration level increases. This is confirmed by the values of Table I, where it becomes clear that the time that the system frequency is below the 49.8-Hz threshold is significantly higher in scenario S25 than in S15 for all the deload levels under study. Both figures show that the implementation of MICAPAS improves the frequency regulation in all scenarios compared to the case without the control. Nevertheless, from Fig. 7, it can be concluded that the deloaded operation in PV-PPs is not justified for low PV penetration levels since their effects on frequency performance are not significant when considering its deviation from the nominal value (50 Hz). On the other hand,
for scenario S25, the system frequency is below 49.8 Hz 36% of

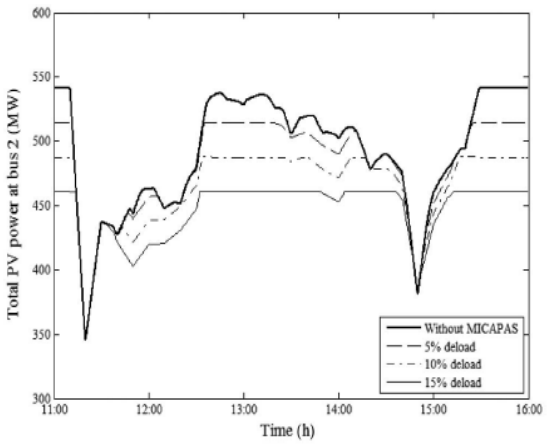

Fig. 9. Aggregated output power of all PV-PPs connected at bus 2 in S25.

the time when the MICAPAS is inactive. The activation of the control significantly improves the frequency regulation in this case. Moreover, as the deload level of the PV arrays increases, the percentage of time that the system frequency is below its threshold decreases. Indeed, when the deload level is 15%, the frequency of scenario S25 remains within its permitted range during the entire simulation range. Considering the economic consequences and security hazards of a poor frequency regulation, the results above lead to the conclusion that for high PV penetration levels, deloaded PVPPs with MICAPAS could be more valuable to the system than maximizing the solar energy itself. Due to the additional costs involved in the deloaded operation, keeping a constant deloadrequirement for PV-PPs all days of the year would not represent a real alternative. Indeed, TSOs should define the conditions which require the activation of the MICAPAS. A reasonable criterion would be requiring its activation only on those days of the year during which the irradiation is expected to have high levels of variability. This could be done based on the MCSI. ,Furthermore, the MICAPAS should only be activated for large PV penetration scenarios.

Fig. 9 depicts the aggregated output power of all PV-PPs connected to bus 2 (see Fig. 5) for the different deload levels considered in scenario S25. Bus 2 includes the largest installed capacity PV resource in this scenario (595 MW).

Fig. 9 also shows how the implementation of the MICAPAS decreases the magnitude of the ramp events experienced by the PV-PPs at the interconnection point. Without MICAPAS, the PV generation connected at bus 2 experiences amaximum value of a 10-min ramp of 196 MW/10-min. With the MICAPAS active with a deload level of 15%, the maximum 10-min ramp decreases by 40%, to 115 MW/10-min.

In order to evaluate the effects of the MICAPAS on the operation of conventional power plants, Figs. 10 and 11 display the duration curve of the power ramps experienced by a 330-MW conventional generator in scenarios S15 and S25, respectively. The (x, y)-coordinate highlighted in Fig. 10 means that 10% of the power ramps experienced by the generator in S15 are larger than 5 MW/10-min.

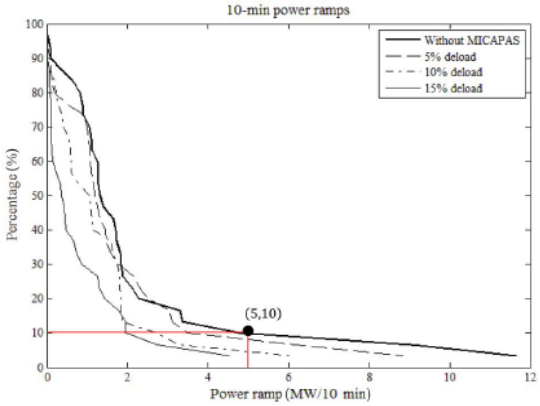

Fig. 10. 10-min power ramps of a 330-MW conventional power plant for S15.

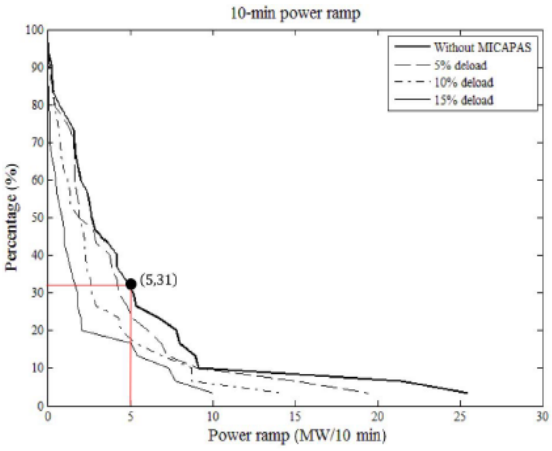

Fig. 11. 10-min power ramps of a 330-MW conventional power plant for S25.

The figures above show that the variability of the PV units due to shading conditions have a direct impact on the magnitude and frequency of the

ramp events experienced by the synchronous generator. As the PV penetration increases, the machine is required to ramp up and down more frequently. While in scenario S15 only 10% of the ramp events are larger than 5 MW/10-min, in S25, 31% exceed this value. The maximum value of the ramp events also increases with the PV penetration: in S15 and S25, this value is equal to 11.6 and 25.5MW/10-min, respectively. The implementation of MICAPAS reduces the ramp requirements on synchronous generators in all scenarios. Consequently, the effectiveness of the control, in terms of reducing the ramp requirements, increases with the deload level. Although not shown here, similar conclusions are obtained for the 5- and 15-min power ramps of the conventional generators.

VII. CONCLUSION

This paper proposed a novel control strategy to allow partially shaded PV-PPs to mitigate the detrimental effects on the power system's frequency. By dividing the PV-PP into *N* sections, the power plant maintains some power reserves by operating them below their optimal operation point (deloaded mode). These reserves are deployed when partial shadowing occurs, thus smoothing the injected power at the connection point of the PV-PP. The proposed control (MICAPAS) was tested in a dynamic model of the power system of Chile for two PV penetration scenarios and different deload levels in the PV-PPs.

The simulation results indicated that the system frequency regulation deteriorates as the PV penetration level increases. In this context, the implementation of MICAPAS in PV-PPs through deloaded operation shows significantly improved frequency regulation in all scenarios under study. However, operating in the deloaded mode imposes an economic burden on the PV-PP's owner and therefore the efficacy of its implementation must be analyzed for each particular case. According to our study, the use of MICAPAS may not be justified for low penetration levels of PV generation since its impacts on the frequency regulation are not significant. However, for high PV levels, the detriment in the frequency regulation of the system would justify the implementation of the proposed control, at least on those days with high irradiance variability. This result is a key issue, particularly in isolated power systems with low inertia and limited frequency control capabilities, since the alternatives to the proposed control may be load-shedding or spilling a significant part of the generated power by the PVPPs due to security reasons. In extreme cases, the network interconnection of new PV projects could be hampered due to security reasons.

Finally, the results have also shown that the magnitude and frequency of the ramp events experienced by the conventional synchronous generators increase considerably with growing PV levels. In this context, the proposed control scheme in the PVPPS was able to reduce the ramp requirements in all considered scenarios. As expected, the reduction becomes more affective as the deloading level in the PV arrays increases.

As future work, it is proposed to evaluate the tradeoff between the system's benefits from the control strategy and the forgone revenues from the deloaded operation. With this in mind, improving the method for forecasting critical days, in terms of fluctuating irradiation, is relevant to minimize the hours of the year operating in deload mode. Once the system's economic benefits are known, compensation structures can be designed as ancillary services.

REFERENCES

[1] A. Mills, *et al.*, "Understanding variability and uncertainty of photovoltaics for integration with the electric power system," Lawrence Berkeley Nat. Lab., Berkeley, CA, USA, Tech. Rep. LBNL-2855E, 2009 [Online]. Available:http://www.osti.gov/scitech/biblio/979812

[2] A. D. Mills and R. H. Wiser, "Implications of geographic diversity for short-term variability and predictability of solar power," in *Proc. IEEE Power Energy Soc. Gen. Meeting*, 2011, pp. 1–9.

[3] North American Electric Reliability Corporation, *Accommodating High Levels of Variable Generation*, North American Electric Reliability Corporation (NERC), Princeton, NJ, USA, 2009 [Online]. Available: http://www.nerc.com/files/ivgtf_report_041609.pdf

[4] D. Lew, G. Brinkman, N. Kumar, S. Lefton, G. Jordan, and S. Venkataraman, "Finding flexibility: Cycling the conventional fleet," *IEEE Power Energy Mag.*, vol. 11, no. 6, pp. 20–32, Nov./Dec. 2013.

[5] J. Eto *et al.*, "Use of frequency response metrics to assess the planning and operating requirements for reliable integration of variable renewable

generation," Lawrence Berkeley Nat. Lab., Berkeley, CA, USA, Rep. LBNL-4142E, 2010.

[6] A. Bidram, A. Davoudi, and R. S. Balog, "Control and circuit techniques to mitigate partial shading effects in photovoltaic arrays," *IEEE J. Photovoltaics*, vol. 2, no. 4, pp. 532–546, Oct. 2012.

[7] M. Z. S. El-Dein, M. Kazerani, and M. M. A. Salama, "Novel configurations for photovoltaic farms to reduce partial shading losses," in *Proc. IEEE Power Energy Soc. Gen. Meeting*, 2011, pp. 1–5.

[8] B. I. Rani, G. S. Ilango, and C. Nagamani, "Enhanced power generation from PV array under partial shading conditions by shade dispersion using Su Do Ku configuration," *IEEE Trans. Sustain. Energy*, vol. 4, no. 3, pp. 594–601, Jul. 2013.

[9] Y. J. Wang and P. C. Hsu, "An investigation on partial shading of PV modules with different connection configurations of PV cells," *Energy*, vol. 36, pp. 3069–3078, 2011.

[10] E. Molenbroek, D. W. Waddington, and K. A. Emery, "Hot spot susceptibility and testing of PV modules," in *Proc. Conf. Rec. 22nd IEEE Photovoltaic Spec. Conf.*, 1991, pp. 547–552.

[11] Q. Zhang, X. Sun, Y. Zhong, and M. Matsui, "A novel topology for solving the partial shading problem in photovoltaic power generation system," in *Proc. IEEE 6th Int. Power Electron. Motion Control Conf. (IPEMC)*, 2009, pp. 2130–2135.

[12] K. Ishaque, Z. Salam, and H. Taheri, and Syafaruddin, "Modeling and simulation of photovoltaic (PV) system during partial shading based on a two-diode model," *Simul. Model. Pract. Theory*, vol. 19, pp. 1613–1626, 2011.